Vision-based system for the control and measurement of wastewater flow rate in sewer systems

L. S. Nguyen, B. Schaeli, D. Sage, S. Kayal, D. Jeanbourquin, D. A. Barry and L. Rossi

ABSTRACT

Combined sewer overflows and stormwater discharges represent an important source of contamination to the environment. However, the harsh environment inside sewers and particular hydraulic conditions during rain events reduce the reliability of traditional flow measurement probes. In the following, we present and evaluate an *in situ* system for the monitoring of water flow in sewers based on video images. This paper focuses on the measurement of the water level based on image-processing techniques. The developed image-based water level algorithms identify the wall/water interface from sewer images and measure its position with respect to real world coordinates. A web-based user interface and a 3-tier system architecture enable the remote configuration of the cameras and the image-processing algorithms. Images acquired and processed by our system were found to reliably measure water levels and thereby to provide crucial information leading to better understand particular hydraulic behaviors. In terms of robustness and accuracy, the water level algorithm provided equal or better results compared to traditional water level probes in three different *in situ* configurations.

Key words | combined sewer overflow, flow measurement, homography, image processing, video monitoring, water level measurement

L. S. Nguyen
B. Schaeli
S. Kayal
D. Jeanbourquin
D. A. Barry
L. Rossi
Ecological Engineering Laboratory (ECOL),
Ecole Polytechnique Fédérale de Lausanne (EPFL),
Lausanne,
Switzerland
E-mail: *laurent.nguyen@epfl.ch*;
basile.schaeli@epfl.ch;
salim.kayal@epfl.ch;
david.jeanbourquin@epfl.ch;
andrew.barry@epfl.ch;
luca.rossi@epfl.ch

D. Sage
Biomedical Imaging Group (BIG),
Ecole Polytechnique Fédérale de Lausanne (EPFL),
Lausanne,
Switzerland
E-mail: *daniel.sage@epfl.ch*

INTRODUCTION

The total pollutant mass carried by sewer systems is an important factor affecting the quality of receiving waters (Burton & Pitt 2002). This is especially the case during large rainfall events where the total amount of wastewater/stormwater exceed the capacity of wastewater treatment plants, in which case combined sewer overflows (CSOs) discharge the excess directly into the natural environment. This untreated water is recognized as an important source of pollution (e.g., Burton & Pitt 2002; Even *et al.* 2006; Burkhardt *et al.* 2007; Chèvre *et al.* 2007; Rossi *et al.* in press). There is little knowledge about the quantity of these discharges although such information would be beneficial, e.g. for environmental assessments. The environmental impact of CSOs depends on the total pollutant mass carried in them, which is estimated from the product of total volumetric flow rate and pollutant concentration. While measurements of the latter are available via sampling and analysis, precise and reliable volumetric flow rate estimations are difficult to obtain, particularly during rain events. Accurate monitoring of the volumetric water flow is thus of crucial environmental importance. In the following, we present and evaluate an *in situ* system for monitoring water flow in sewers.

Determination of the volumetric water discharge Q requires knowledge of water velocity at each point in a given cross-section:

$$Q = \int\int_S v_N(\bar{S})\mathrm{d}\bar{S} = SV_m[m^3/s]. \quad (1)$$

where v_N is the normal velocity and S is the cross-sectional area. In Equation (1) it has been assumed that the integrals

doi: 10.2166/wst.2009.659

can be approximated by the product of S and the mean normal velocity V_m. Next, V_m is further assumed to equal the surface water velocity V_S factored by μ, a scalar that depends on the nature of the channel (material, shape, etc.), the water level and the measurement position (Larrarte 2006):

$$V_m = \mu V_S [m/s]. \quad (2)$$

The section S is defined as $S = P(h)$ $[m^2]$ where P is the function describing the water channel geometric profile and h $[m]$ is the water level. In practice, the channel profile P is known from engineering drawings or *in situ* measurements. The combination of Equation (1) and Equation (2) give the channel flux as:

$$Q = \mu P(h) V_S \quad (3)$$

The knowledge of the water level h is required to measure Q. Various devices are available for measuring water level in sewers. Pressure transducers are widely used and are placed on the base of the sewer channel. The water level is inferred from pressure measurements (Jensen 2004). While their application in clean water has been demonstrated, their use in sewers is still problematic as they become quickly clogged by the solid material contained in the flow and thereby require frequent maintenance. During significant flows, such probes can be torn away. Ultrasonic probes, placed outside of the flow, are another way to measure the water level. They are unaffected by clogging and their robust design makes them well-suited for harsh environments. However, pressure transducers and ultrasonic probes both provide localized measurements which are not able to characterize effects such as hydraulic jumps. Moreover, these devices do not give any indication of reliability of the measurements.

Video cameras enable robust monitoring of wastewater flow discharge. As they are placed above the water, clogging and instrument loss are avoided. They allow measurements of a relatively large surface and maintenance needs are low. Finally, they open the possibility for identification and measurement of particular hydraulic behaviors by means of image visualization, thus providing a better understanding of the hydraulics of sewer systems and CSOs in particular.

Different approaches to image-based water level measurement have been proposed. Takagi *et al.* (1998) proposed a method for detecting water level using the reflection or diffraction of a metal ruler in the water. Iwahashi & Udomsiri (2007) proposed a system for water level measurement in rivers based on the assumption that the land region is significantly more structured than the water region. This is not the case in sewer systems, especially during rain events where the flow is very energetic. Konaré *et al.* (2003) presented an image-processing algorithm based on edge detection; however, it has not been tested in real conditions. In these papers, the correction of distortion due to the perspective was not taken into account; the camera must then be placed orthogonally to the filmed scene. Due to the limited space inside sewer structures, it is not possible to meet these requirements in general.

We present here a new system for online monitoring of sewers based on image processing techniques, and show its application to measure water height in sewers. This vision-based tool opens new horizons for the robust real-time assessment of diverse hydraulic structures. In this paper, we focus on the system architecture and the water level measurement algorithm; the surface water velocity algorithm will be presented in an upcoming article.

METHODOLOGY

System requirements

The requirements for a robust vision-based system for monitoring sewers were defined as follows: visual analysis of hydraulic behavior, on-line water level and water velocity measurements, automatic alarm system for particular events (overflows, flood risks, etc.), database for data management (images, events, measurements, etc.), remote configuration and efficient data visualization. Combined with the accessibility issues and the difficult conditions within sewer systems, these requirements formed the design specification for the hardware and software selection of the vision-based system. The monitoring system must also be able to take measurements autonomously for long periods of time with minimum maintenance.

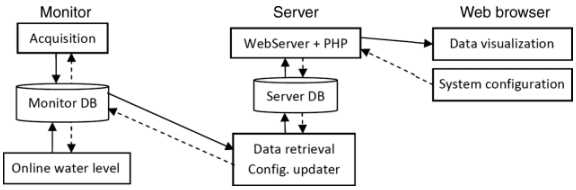

Figure 1 | View of the system components. Lines represent the flow of information from the monitor to the user's web browser. Dashes represent configuration of the system parameters, from the user to the video acquisition service and algorithms.

System architecture

The software architecture is a *multi-tier* configuration where every monitoring site (called hereafter a *monitor*) is accessed through a server (Figure 1). A web-based user interface enables configuration of the cameras and the parameters of the image-processing algorithms. Images and videos acquired by the cameras are stored within the local database (DB). A service implementing the algorithms described below using National Instrument LabVIEW periodically monitors the local database and processes the newly captured data (images). This architecture offers the possibility of deploying various online image processing algorithms in parallel, each of them getting their configuration data from the local database and feeding their results into it.

The architecture was designed to cover two possible communication scenarios. If reliable network connectivity (wired or wireless) is available on the monitored site, the monitoring computer is placed in a dry remote location. When no internet connection is available, the computer is contained inside a waterproof box inside the CSO; the communication is assured by a UMTS modem. Since communications between the monitor and the server may be unreliable, all acquired media and computation results are stored locally on the monitors. An asynchronous service running on the server is responsible for sending configuration information and retrieving results.

A web-based user interface is used to display the computation results. Images and videos are retrieved from the monitor on demand, in which case a copy is stored on the central server for future analysis. The measurement data are processed on the server in order to generate alarms when meaningful events occur. The system accepts other input like measurement devices such as ultrasonic probes, temperature sensors or rain measurement devices. The infrastructure is supported by the Apache web server with PHP modules and a PostgreSQL database. The server-monitor synchronization and image acquisition is performed by custom Java software.

Camera cases are 100% waterproof and corrosion resistant, and long life, low-power and water-resistant infra-red LED illumination devices are used. In contrast to visible light, infrared has the benefit of not attracting insects. We use PoE (Power over Ethernet) IP cameras, which enables both power and data to go through the same Ethernet cable and have standard connectors. This latter consideration makes the system independent of a specific camera manufacturer.

The total cost of the prototype including software licenses and hardware equipment is approximately US$11K which is moderate in comparison to other flow monitoring systems, making future industrial deployment of the system realistic.

Water level measurement

As described in the introduction, the water level h is necessary for the determination of the volumetric flow rate Q. The image-based water level algorithm identifies the wall/water interface from sewer images and measures its position with respect to real world coordinates. The image analysis consists in three steps: pre-processing, calibration and line detection.

Step 1: pre-processing

The acquired images have a low Contrast-to-Noise Ratio (CNR), typically around 3:

$$CNR = |m_{\text{wall}} - m_{\text{water}}|/s_N. \quad (4)$$

where m_{wall} and m_{water} are respectively the mean pixel intensities of the wall and the water; s_N is the standard deviation of the noise. The reasons of this low quality are (i) noise due to the low illumination, (ii) high rate of video compression and (iii) the presence of tiny water particles in the air.

The goal of the pre-processing step is to enhance the pertinent features of the image, the edges between the water and the wall. The following steps were implemented to perform this: the original image are first denoised using a Gaussian filter, then a Sobel gradient transformation is applied given a gradient vector $\{G(u,v),\ \theta(u,v)\}$ at every coordinates (u,v). A procedure gives favor to the vertical gradient directions $\theta_{\vdash}$. It uses a tuning parameter γ (typically for our level of noise and our resolution, we set γ to 5):

$$G_{\text{enhanced}}(u,v) = |\cos(\theta(u,v) - \theta_{\vdash})|^{\gamma} G(u,v)$$
$$\text{with } \theta(u,v) = \tan^{-1}\left(\frac{G_y(u,v)}{Gx(u,v)}\right) \tag{5}$$

Finally, the last step of the pre-processing stage uses a thresholding operation to convert the enhanced directional gradient image to a binary image (the threshold is usually set to 10% of the maximum value).

Step 2: calibration

Calibration is necessary to make accurate image-based measurements. The goal of this step is to transfer points from the image coordinate system (u,v) in pixels [px] to a world coordinate system (X_W, Y_W, Z_W) in meters [m]. Calibration can be separated into two parts. First, intrinsic calibration deals with the internal parameters of the camera. The camera model used for intrinsic calibration here is the central projection model, also known as the pinhole camera model (e.g., Tsai 1987; Heikkila & Silven 1997). Intrinsic parameters relate the 3D camera coordinate system (X_C, Y_C, Z_C) [m] to the pixel image coordinate system (u,v) [px]:

$$s\begin{bmatrix} u \\ v \\ 1 \end{bmatrix} = \begin{bmatrix} a_u & a_s a_u & u_0 & 0 \\ 0 & a_v & v_0 & 0 \\ 0 & 0 & 1 & 0 \end{bmatrix} \begin{bmatrix} X_C \\ Y_C \\ Z_C \\ 1 \end{bmatrix} = \begin{bmatrix} I_C & 0_{1\times 3} \end{bmatrix} \begin{bmatrix} X_C \\ Y_C \\ Z_C \\ 1 \end{bmatrix} \tag{6}$$
$$\text{with } a_u = -k_u f \text{ and } a_v = k_v f.$$

The intrinsic matrix I_C contains all the intrinsic parameters: k_u and k_v are scaling factors in the horizontal and vertical directions respectively [px/m]; α_s is the skew coefficient, defining the angle between the horizontal and vertical axes of a pixel in the camera's CCD sensor; u_0 and v_0 are the image coordinates [px] of the optical center projection and f is the focal length [m]. Intrinsic parameters are estimated using the Matlab camera calibration toolbox (Bouguet 2008). In our tests, using in the order of 20 input images led to calibration error of less than one pixel.

Once the intrinsic parameters are identified, we must perform the extrinsic calibration to relate the camera position with respect to the filmed scene. The tri-dimensional transformation between the camera coordinate system (X_C, Y_C, Z_C) and the world coordinate system (X_W, Y_W, Z_W) is achieved through a rotation R and a translation T. The combination of R and T forms the extrinsic matrix A:

$$\begin{bmatrix} X_C \\ Y_C \\ Z_C \\ 1 \end{bmatrix} \begin{bmatrix} r_{11} & r_{12} & r_{13} & t_x \\ r_{21} & r_{22} & r_{23} & t_y \\ r_{31} & r_{32} & r_{33} & t_z \\ 0 & 0 & 0 & 1 \end{bmatrix} \begin{bmatrix} X_W \\ Y_W \\ Z_W \\ 1 \end{bmatrix}$$
$$= \begin{bmatrix} R_{3\times 3} & T_{1\times 3} \\ 0_{3\times 1} & 1_{1\times 1} \end{bmatrix} \begin{bmatrix} X_W \\ Y_W \\ Z_W \\ 1 \end{bmatrix} = A_{4\times 4} \begin{bmatrix} X_W \\ Y_W \\ Z_W \\ 1 \end{bmatrix}. \tag{7}$$

The relation between the image coordinates and the world coordinates can be obtained combining Equation (6) and Equation (7):

$$s\begin{bmatrix} u \\ v \\ 1 \end{bmatrix} = \begin{bmatrix} I_{C,3\times 3} & 0_{1\times 3} \end{bmatrix} A_{4\times 4} \begin{bmatrix} X_W \\ Y_W \\ Z_W \\ 1 \end{bmatrix}. \tag{8}$$

Assuming that the filmed scene is a planar surface, Equation (8) can be simplified. Indeed, the plane can be parameterized as $Z_W = 0$; thus every point located on this planar surface have the form $(X_W, Y_W, 0)$. The resulting transformation is known as a homography (Estrada *et al.* 2004):

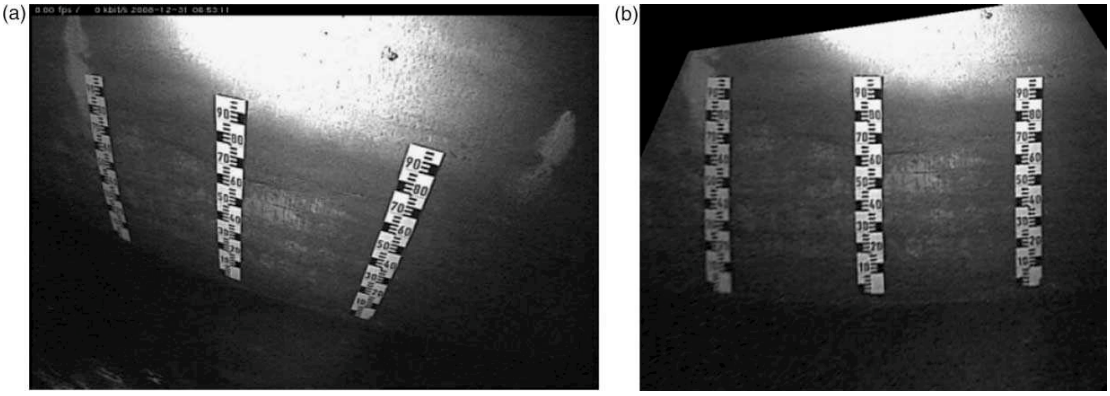

Figure 2 | Rectification of the perspective distortion using the homography transformation: (a) original image; (b) rectified image; the homography matrix was computed with values from the rulers; lens distortion correction was applied.

$$s\begin{bmatrix} u \\ v \\ 1 \end{bmatrix} = \begin{bmatrix} I_{C,3\times3} & 0_{1\times3} \end{bmatrix} A_{4\times4} \begin{bmatrix} X_W \\ Y_W \\ 0 \\ 1 \end{bmatrix} = \begin{bmatrix} a_u & a_s a_u & u_0 \\ 0 & a_v & v_0 \\ 0 & 0 & 1 \end{bmatrix} \begin{bmatrix} r_{11} & r_{12} & t_x \\ r_{21} & r_{22} & t_y \\ r_{31} & r_{32} & t_z \end{bmatrix} \begin{bmatrix} X_W \\ Y_W \\ 1 \end{bmatrix} = H \begin{bmatrix} X_W \\ Y_W \\ 1 \end{bmatrix}, \quad \text{if } Z_W = 0. \tag{9}$$

The H matrix describes the linear transformation relating two projective planes, in our case the camera plane and the filmed planar surface. The homography maps any point of the sewer wall from image coordinates (u,v) [px] to world coordinate (X_W, Y_W) [m] and vice versa, thereby allowing metric measurements on images.

Since we do not know R and T, we estimate the homography matrix H by the optimization algorithm described in (Soatto *et al.* 2005). The user needs to manually specify the (X_W, Y_W) coordinates of multiple pixels of the original image. The algorithm needs a minimum of 4 such *correspondence points* to estimate H. Since both the selection of a pixel and the attribution of a (X_W, Y_W) coordinate are subject to small errors, increasing the number of points yields more accurate results. In our test images, choosing 20 correspondence points reduced the error such that the u coordinates of the vertical edges of each rulers differed by less than one pixel on average. An example of the application of the homography matrix to an image is displayed in Figure 2.

Note that the identification of the intrinsic and extrinsic calibration parameters only needs to be performed once when a camera is installed at a new site.

Step 3: line detection

The goal of the line detection algorithm is to extract the wall/water interface from sewer images. Assuming the sewer wall and the water to be planar surfaces, the interface is a straight line. We use the Hough transform (Duda & Hart 1972) to detect the wall/water interface. The method involves transforming each pixel point of the image (u,v) to a vector of parameters $(\lambda_1, \ldots, \lambda_n)$, known as the *Hough space*. The Hough space is defined by the parameterization defining the geometric pattern. Each pixel in the image adds its contribution to the n-dimensional *accumulator array*. The location of a peak value in the accumulator array gives values of the parameters $(\lambda_1, \ldots, \lambda_n)$, enabling the unequivocal representation of the geometric pattern. Since in our case the feature to be extracted is a straight line, two parameters (the slope and the intercept) are necessary to represent it mathematically. We therefore use the parametric representation $(\lambda_1 = a, \lambda_2 = h)$ in the world coordinate system (X_W, Y_W).

The implementation of the complete water level algorithm is illustrated below (Figure 3).

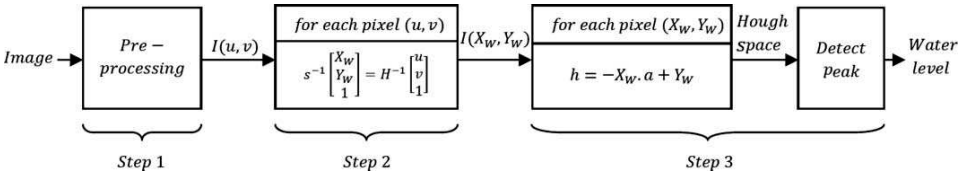

Figure 3 | Flowchart of the complete water level algorithm.

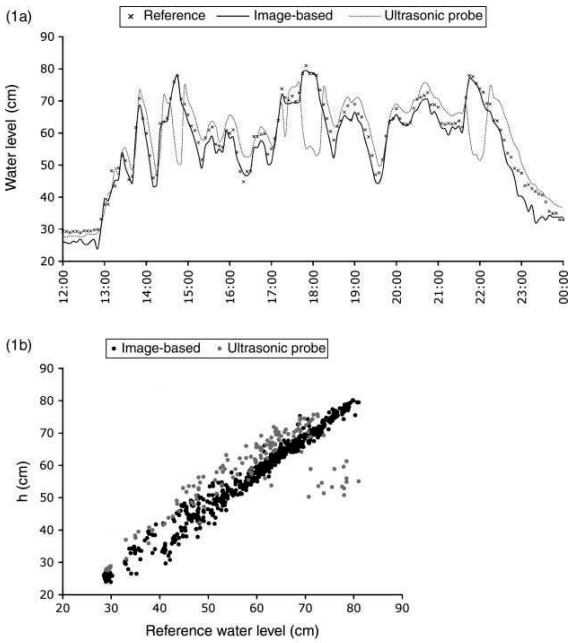

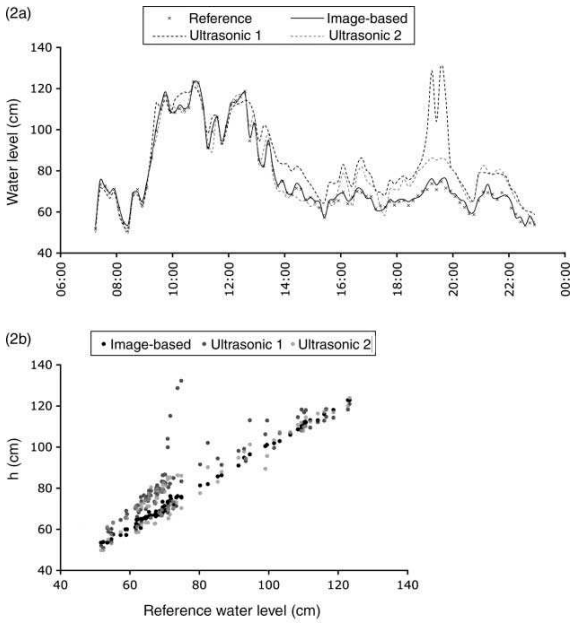

Figure 4 (*continued*)

Figure 4 (*continued*)

In practice, the assumption of the wall/water interface being a straight line is in many cases unverified due to the hydraulic turbulences present in the sewer systems. The algorithm described in this section is however robust enough to withstand waves in the water channel. The computation time for the whole water level algorithm is approximately of 400 ms on an Intel Core 2 Duo at 2.13 GHz for original images of size 640×480 and Hough space of size 50×50.

RESULTS AND DISCUSSION

We have conducted long-term conclusive *in situ* tests of the vision-based system in various sewer configurations (CSOs, stormwater sewerage and wastewater treatment plants). In order to validate the image-based system, we have put classical sensors (ultrasonic or pressure probes) into the CSO and we have manually recorded the water level visible on the wall-mounted rulers. This last measurement serves as ground-truth reference. Offline water level processing was conducted on images collected during rain events in various sewer structures to validate our approach.

The first system was installed inside CSO in Lausanne, Switzerland (Figure 4.1c). The operators had little understanding of its hydraulic behavior; in particular, they could not determine if an overflow would occur during a rain event. Sewer images provided information on the duration and intensity of the overflows; the system therefore contributed to better understand the behavior of this structure. An ultrasonic probe (Teledyne ISCO 4210) was also installed in the CSO to monitor the water level. The classical water level probes tend to reproduce the same behavior; however in several cases they provide singular results. In Figure 4.1a, the ISCO probe outputs false

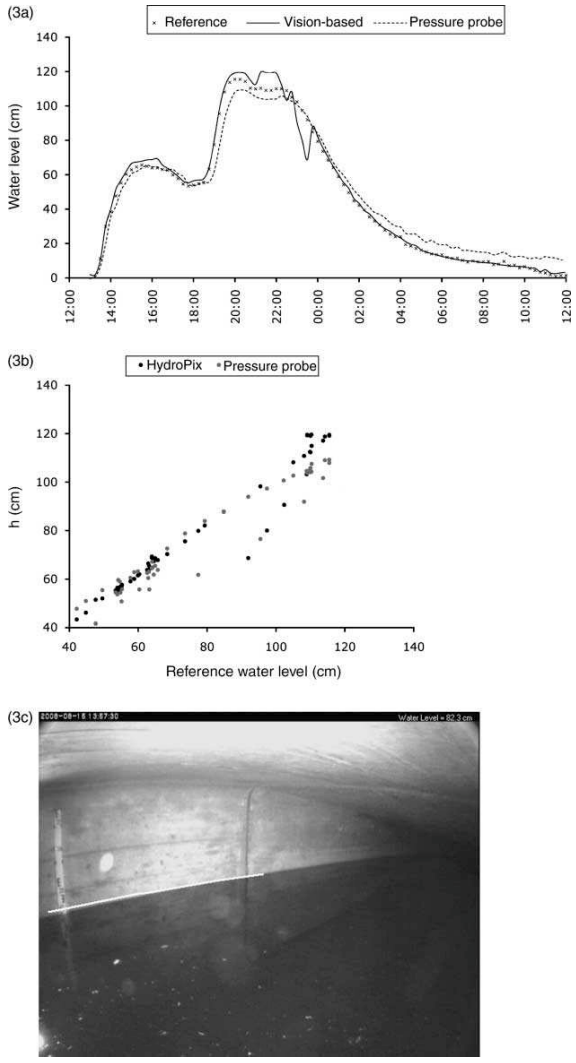

Figure 4 | Water level algorithm results during rain events in various sewer configurations: (1) and (2) are two CSOs in the city of Lausanne, Switzerland; (3) is stormwater sewerage near Zürich, Switzerland. Comparison of the water level algorithm with: one ultrasonic probe in (1); two ultrasonic probes placed at an approximate separation distance of 1.5 m in (2); one pressure probe in (3). (a) displays the water level reference and measurements (image-based algorithm and ultrasonic or pressure) with time. (b) plots the measured water levels with respect to the water level reference. (c) shows one image used for the detection of the water line in the CSO.

measurements for high water levels at 15:00, 18:00 and 22:00. The reason is that the relatively small size of the CSO requires the probe to be placed too close to the water; for high water levels, it leaves its working range. We should note that the probe was installed by the engineers of Lausanne's sewer department following their regular procedures, and taking in account the physical constraints of the CSO. In contrast, the measurements provided by the image-based water level algorithm proved to be very close to the reference values. The root mean square error (RMSE) between the ground-truth and the vision-based system is 2.96 cm.

The second system was also installed in a CSO in Lausanne, Switzerland (Figure 4.2c) with two ultrasonic probes (Teledyne ISCO 4210) set up at a distance of 1.5 m. It was observed that the two probes provided different results during rain events. In this experiment, the RMSE is 1.33 cm between the ground-truth and the vision-based system. After carefully visual analysis of the images, the cause of the discrepancies between the measurements was identified as a hydraulic jump. In Figure 4.2a, ultrasonic probe 1 gives a difference of 60 cm; however, the cause of this discrepancy is unexplained, as far we know.

A third test took place in a stormwater sewer near Zürich, Switzerland (Figure 4.3c). During rain events, flow estimations based on water level measurements from an ultrasonic probe provided results that were much greater than what had been expected based on computer simulations. The acquired images revealed that water flow traveled upstream. Further investigation revealed that the water level in the sewer increased because of back flow of the receiving water (a small river) into the sewage system. This phenomenon was discovered thanks to the recorded images. The RMSE of the image-based system compare to the reference is 4.61 cm.

In the last two cases, the images greatly improved the understanding of particular hydraulic behaviors like hydraulic jumps or upstream flow. The image-based system provides an online accurate measurement device without any contact and gives access to off-line investigations on the behavior of the water flow.

The described system provides a good estimation of the water level and more video showing the relevant events (discharge). The videos provide information about both the duration and the extent of water discharges. Coupling such information with the rain level greatly helps to understand the behavior of a given CSO.

CONCLUSIONS

We showed that video images provide valuable information for monitoring harsh environments such as sewer systems. Three-months *in situ* tests demonstrated the robustness of the vision-based system. Images acquired and processed by our system were found to reliably measure water levels and thereby to provide crucial information leading to a better understanding of particular hydraulic behavior. In terms of robustness and accuracy, the water level estimation provided equal or better results compared to traditional water level probes in three different *in situ* configurations. Moreover, in contrast to ordinary probes, images enable human beings to verify the outputs of the algorithms; this was proved to be very useful in the case of erratic data.

The robust design of the hardware equipment successfully withstood the harsh environment within sewer structures for long periods. The system architecture allows a flexible and modular implementation for various communication scenarios. The software structure was designed in such a way that an arbitrary number of traditional probes and diverse image-based algorithms can be plugged to the system easily, making the system a complete on-line monitoring tool for hydraulic structures.

Finally, we remark that, in terms of decision making, images are very helpful in describing the issues concerning stormwater management to non-specialists.

ACKNOWLEDGEMENTS

The authors thank the Swiss Commission for Technology and Innovation (KTI/CTI CTI 8934.1 PFIW-IW) for financial support, the Etrinex SA Company (industrial partner of the project), Dr M. Burkhardt (Eawag) for providing the near Zürich information and the City of Lausanne for their help in conducting measurements in the sewer system of the city.

REFERENCES

Bouguet, J. Y. 2008 Camera Calibration Toolbox for Matlab. http://www.vision.caltech.edu/bouguetj/calib_doc/ (accessed 2009-05-19).

Burkhardt, M., Kupper, T., Hean, S., Schmid, P., Haag, R., Rossi, L. & Boller, M. 2007 Release of Biocides from Urban Areas into Aquatic Systems. *Sixth International Conference on Sustainable Techniques and Strategies in Urban Water Management (NOVATECH)*, Lyon, France, Vol. 3, pp. 1483–1489.

Burton, G. A. & Pitt, R. E. 2002 *Stormwater Effects Handbook: A Toolbox for Watershed Managers, Scientists and Engineers*. Lewis Publishers, Boca Raton.

Chèvre, N., Vallotton, N. & Rossi, L. 2007 Risk Assessment of Urban Runoff Pollution in Rivers: How to Deal with Time-Varying Concentrations? *Sixth International Conference on Sustainable Techniques and Strategies in Urban Water Management (NOVATECH)*, Lyon, France, Vol. 3, pp. 1367–1374.

Duda, R. O. & Hart, P. E. 1972 Use of the hough transformation to detect lines and curves in pictures. *Comm. ACM* **15**(1), 11–15.

Estrada, F. J., Jepson, A. D. & Fleet, D. 2004 Planar Homographies. Lecture notes, http://www.cs.utoronto.ca/ ~ strider/vis-notes/tutHomography04.pdf (accessed 2009-05-19).

Even, S., Mouchel, J.-M., Servais, P., Flipo, N., Poulin, M., Blanc, S., Chabanel, M. & Paffoni, C. 2006 Modelling the impacts of combined sewer overflows on the river seine water quality. *Sci. Total Environ.* **375**(1–3), 140–151.

Heikkila, J. & Silven, O. 1997 A Four-Step Camera Calibration Procedure with Implicit Image Correction. *1997 IEEE Computer Society Conference on Computer Vision and Pattern Recognition (CVPR'97), 1106*.

Iwahashi, M. & Udomsiri, S. 2007 Water Level Detection from Video with FIR Filtering. *Proceedings of the 16th International Conference on Computer Communication and Networks*, pp. 826–831.

Jensen, K. D. 2004 Flow measurements. *J. Braz. Soc. Mech. Sci. Eng.* **26**(4), 400–419.

Konaré, D., Pierre, S., Weng, J. Y. & Morand, E. 2003 Real-time image processing for remote sensing. *Can. Conf. Electrical Comput. Eng.* **2**, 699–702.

Larrarte, F. 2006 Velocity fields within sewers: an experimental study. *Flow Meas. Instrum.* **17**(5), 282–290.

Rossi, L., Chèvre, N., Fankhauser, R. & Krejci, V. in press Probabilistic Environmental Risk Assessment of Urban Wet-Weather Discharges: an Approach Developed for Switzerland. *Accepted for publication in Urban Water Journal*.

Soatto, S., Yi, M., Kosecka, J. & Sastry, S. 2005 *An Invitation to 3D Vision: from Images to Mathematic Models*. Springer-Verlag New York Inc, New York, NY, section 5.3, pp. 131–142.

Takagi, Y., Tsujikawa, A., Takato, M., Saito, T. & Kaida, M. 1998 Development of a non contact liquid level measuring system using image processing. *Water Sci. Technol.* **37**(12), 381–387.

Tsai, R. Y. 1987 A versatile camera calibration technique for high-accuracy 3D machine vision metrology using off-the-shelf tv cameras and lenses. *IEEE J. Robot. Autom.* **3**(4), 323–344.